Journal of Physiology (1992), **456**, *pp.* 425–441
With 12 figures
Printed in Great Britain

VOLTAGE-DEPENDENT SODIUM AND CALCIUM CURRENTS IN CULTURED PARASYMPATHETIC NEURONES FROM RAT INTRACARDIAC GANGLIA

BY Z.-J. XU AND D. J. ADAMS*

From the Department of Molecular and Cellular Pharmacology, University of Miami School of Medicine, Miami, FL 33101, USA

(*Received 28 October 1991*)

SUMMARY

1. Depolarization-activated Na^+ and Ca^{2+} currents underlying the rising phase of the action potential in mammalian parasympathetic ganglion cells were investigated in voltage-clamped neurones dissociated from neonatal rat intracardiac ganglia and maintained in tissue culture.

2. A current component isolated by replacing intracellular K^+ with Cs^+ or arginine and adding 0·1 mM Cd^{2+} to the external solution was dependent on extracellular [Na^+] and reversibly blocked in the presence of 300 nM tetrodotoxin (TTX). Peak amplitudes of Na^+ currents elicited by step depolarization from a holding potential of −100 mV were 351 ± 18 pA/pF (140 mM extracellular Na^+).

3. The sodium current–voltage (*I–V*) curve exhibited a threshold for activation at −40 mV and reached a maximum at −10 mV. The Na^+ conductance increased sigmoidally with increasing depolarization reaching half-maximal activation at −25 mV, with a maximum slope corresponding to 7·5 mV per e-fold change in conductance.

4. During a maintained depolarization, Na^+ currents turned on and then decayed (inactivated) with an exponential time course. The time constant of inactivation was voltage dependent decreasing from 0·85 ms at −20 mV to 0·3 ms at +60 mV (23 °C). The steady-state inactivation of the Na^+ conductance was voltage-dependent with half-inactivation occurring at −61 mV and near-complete inactivation at −20 mV. Recovery from inactivation also followed an exponential time course with a time constant that increased at depolarized membrane potentials.

5. A voltage- and Ca^{2+}-dependent current was isolated by replacement of intracellular K^+ with either Cs^+ or arginine and of extracellular Na^+ with tetraethylammonium and the addition of TTX. Extracellular Ba^{2+} or Na^+ (in the absence of external divalent cation) could substitute for Ca^{2+}. Peak Ca^{2+} current increased with increasing extracellular [Ca^{2+}] and above 10 mM ($K_d \approx 4$ mM) approached saturation. The peak Ca^{2+} current density was 45 ± 4 pA/pF (2·5 mM-extracellular Ca^{2+}).

6. The Ca^{2+} *I–V* relation exhibited a high threshold for activation (−20 mV) and

* To whom correspondence should be addressed.

MS 9850

reached a maximum at +20 mV. Changing the holding potential from −100 to −40 mV did not alter the *I–V* relationship. Peak Ca^{2+} conductance increased sigmoidally with increasing depolarization reaching half-maximal activation at −4 mV, with a maximal slope of 4 mV per e-fold change in Ca^{2+} conductance.

7. The kinetics of activation and inactivation of the Ca^{2+} current were voltage dependent and the time course of inactivation was fitted by the sum of two exponentials. The time to peak of the inward Ca^{2+} current decreased with increasing depolarization. With maintained depolarization the Ca^{2+} current slowly inactivated, by about 50% during a 400 ms pulse. Steady-state inactivation of the Ca^{2+} current was voltage dependent with half-inactivation occurring at −38 mV and complete inactivation at 0 mV. The rate of recovery from inactivation increased with hyperpolarization with both time constants reduced e-fold by a 60 mV hyperpolarization.

8. Calcium currents were inhibited reversibly in a dose-dependent manner by external Cd^{2+}, with half-maximal inhibition at 3·6 μM. The peak amplitude of the Ca^{2+} current was increased 21% by 5 μM Bay K 8644, and was inhibited by 5 μM nifedipine applied extracellularly. Raising the nifedipine concentration to ⩾ 30 μM produced maximal inhibition of 67%.

9. The Ca^{2+} current was inhibited irreversibly by ~ 70% by bath application of a maximally effective dose of ω-conotoxin (ω-CGTX; 300 nM). The residual current in ω-CGTX was further inhibited by ~ 50% by 20 μM nifedipine. The ω-CGTX- and dihydropyridine-resistant current was inhibited by Cd^{2+}, suggesting that rat parasympathetic neurones contain at least three pharmacologically distinct types of calcium channel.

INTRODUCTION

Depolarization-activated sodium and calcium currents underlie neuronal excitability and neurotransmission in the central and peripheral nervous systems. Characterization of the biophysical and pharmacological properties of Na^+ and Ca^{2+} currents is essential for understanding the contribution of these currents to the action potential and the different firing patterns observed in intracardiac neurones of the mammalian heart (Allen & Burnstock, 1987; Seabrook, Fieber & Adams, 1990; Xi, Thomas, Randall & Wurster, 1991).

A variety of voltage-dependent Na^+ currents have been found in mammalian sympathetic neurones (Belluzzi & Sacchi, 1986; Schofield & Ikeda, 1988) and sensory neurones (Kostyuk, Veselovsky & Tsyndrenko, 1981*b*; Ikeda, Schofield & Weight, 1986). In rat sensory neurones, a tetrodotoxin (TTX)-sensitive and TTX-resistant component in the Na^+ current have been described (Kostyuk *et al.* 1981*b*; Ikeda *et al.* 1986; Ikeda & Schofield, 1987). Similarly, several different types of voltage-dependent Ca^{2+} currents have been identified in mammalian autonomic ganglion cells (Marrion, Smart & Brown, 1987; Schofield & Ikeda, 1988; Hirning, Fox, McCleskey, Olivera, Thayer, Miller & Tsien, 1988; Belluzzi & Sacchi, 1989) and sensory neurones (Kostyuk, Veselovsky & Fedulova, 1981*a*; Bossu, Feltz & Thomann, 1985; Fedulova, Kostyuk & Veselovsky, 1985; Bossu & Feltz, 1986; Ikeda *et al.* 1986; Carbone & Lux, 1987; Kostyuk, Shuba & Savchenko, 1988). The characteristics of high-threshold depolarization-activated Ca^{2+} currents have been

described in rat sympathetic neurones (Hirning *et al.* 1988; Schofield & Ikeda, 1988; Belluzzi & Sacchi, 1989) and, in addition, a low-threshold Ca^{2+} current has been reported in rabbit pelvic parasympathetic neurones (Akasu, Tsurusaki & Tokimasa, 1990; Tsurusaki, Nishimura & Akasu, 1990).

Although a description of voltage-dependent Na^+ and Ca^{2+} currents in parasympathetic neurones isolated from the interatrial septum of bullfrog heart has recently appeared (Clark, Tse & Giles, 1990), there has been no examination, to date, of these currents in mammalian parasympathetic cardiac neurones. In this study, cultured neurones dissociated from parasympathetic cardiac ganglia in neonatal rat atria are used to examine the depolarization-activated Na^+ and Ca^{2+} conductances of cardiac ganglion cells. A preliminary report of some of these results has been published (Adams & Xu, 1989).

METHODS

Voltage-clamp recordings using the whole-cell patch-clamp technique were made from cultured neurones dissociated from neonatal rat parasympathetic cardiac ganglia. The preparation of cultured intracardiac neurones and electrophysiological recording methods were described in the preceding paper (Xu & Adams, 1992). The extracellular physiological salt solution (PSS) was of the following ionic composition (mM): 140 NaCl, 3 KCl, 2·5 $CaCl_2$, 0·6 $MgCl_2$, 7·7 D-glucose, 10 HEPES, adjusted to pH 7·4 with NaOH. Outward K^+ currents were abolished by isotonically substituting K^+ with Cs^+ or arginine in the patch electrode and Na^+ with tetraethylammonium (TEA) in the external solution. Extracellular Ca^{2+} concentration (2·5–25 mM) was varied by replacement of NaCl or TEACl with an osmotically equivalent amount of $CaCl_2$. Patch electrodes were filled with an intracellular solution containing 100 mM CsCl, 10 mM-Cs_4EGTA or Cs_4BAPTA, 2 mM Mg_2ATP, and 40 mM HEPES-CsOH; pH 7·2 at 22 °C. Corrections for liquid junction potentials between the bath solution and indifferent electrode (0·15 M KCl agar bridge) were made with respect to a reference electrode (saturated KCl, reverse sleeve junction; Corning X-EL 47619).

Solutions were made from analytical grade reagents. Arginine chloride, EGTA and TEACl were obtained from Sigma Chemical Co. (St Louis, MO, USA), $CdCl_2$ and CsCl from Aldrich Chemical Co. (Milwaukee, WI, USA), BAPTA from Molecular Probes Inc. (Eugene, OR, USA), amlodipine maleate from Pfizer Ltd (Sandwich, Kent, UK), and tetrodotoxin (TTX), nifedipine, (±) Bay K 8644, amiloride hydrochloride and ω-conotoxin, GVIA (ω-CGTX) from Calbiochem Corp. (San Diego, CA, USA). Dihydropyridine compounds, nifedipine and (±) Bay K 8644, were dissolved in ethanol as a 5 mM stock solution and added to the bath solution to give the final concentrations stated. Application of 0·5% ethanol alone had no effect on the depolarization-activated Ca^{2+} currents studied.

Calcium current amplitudes tend to decline over the course of whole-cell voltage-clamp experiments (Kostyuk *et al.* 1981*a*; Fenwick, Marty & Neher, 1982). This 'run-down' phenomenon, during which Ca^{2+} current declines slowly during the initial 20–60 min of recording, has been described in detail for vertebrate neurones (Kostyuk *et al.* 1981*a*; Forscher & Oxford, 1985). Addition of EGTA and MgATP to the pipette solution tends to slow current run-down (Fedulova *et al.* 1985; Forscher & Oxford, 1985). In our experiments with 1–10 mM EGTA or BAPTA and 2 mM ATP present in the pipette, a decline of Ca^{2+} current was also observed. It was described by the sum of two exponentials: the amplitude decreased by ~ 25% within 10 min after breaking into the cell (τ_{fast} = 4·2 min) and then declined more slowly (τ_{slow} = 500 min). Ca^{2+} currents were recorded between 10 and 40 min after formation of the whole-cell configuration, during which run-down of I_{Ca} was < 10%. Ca^{2+} currents recorded within this interval were used for quantitative analysis.

Averaged data are represented as means ± standard error of the mean (S.E.M.).

RESULTS

As described in the preceding paper (Xu & Adams, 1992), the rising phase and overshoot of the action potential are due to an influx of Na^+ and Ca^{2+} and the repolarization and after-hyperpolarization are due mainly to the outward K^+

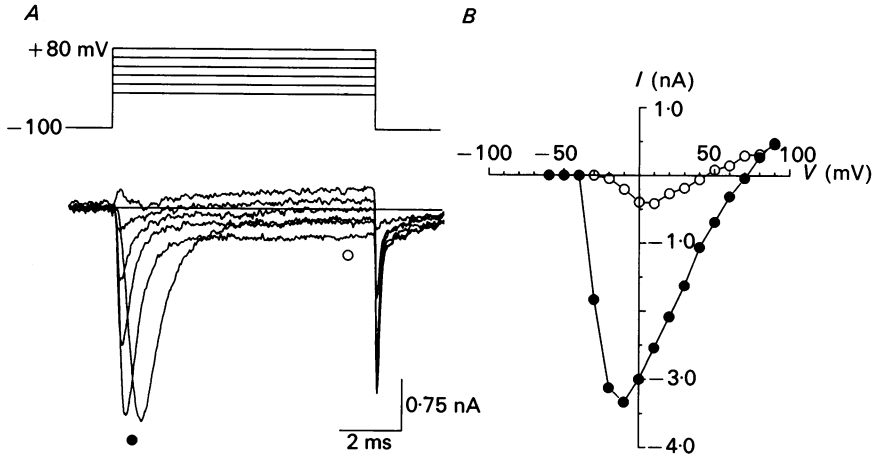

Fig. 1. Depolarization-activated inward currents in cultured neurones dissociated from rat intracardiac ganglia. *A*, whole-cell, inward currents recorded in normal PSS in response to voltage steps in 20 mV increments from −20 to +80 mV from a holding potential of −100 mV. The pipette solution contained 10 mM Na^+ and K^+ was replaced isotonically by arginine. *B*, current–voltage (*I–V*) relations for the peak (●) and sustained (○) currents elicited by voltage steps of 10 mV increments from −60 to +90 mV in the same cell as shown in *A*.

movement. When outward K^+ currents were blocked by replacing K^+ by arginine in the patch pipette, depolarization of the soma membrane from a holding potential of −100 mV to potentials more positive than −30 mV induced a rapid inward current followed by a slow inward current (Fig. 1*A*). The transient component was blocked by TTX (300 nM) and the sustained current was blocked by 0·1 mM Cd^{2+} (not shown). The *I–V* relations for the peak and the sustained inward currents (Fig. 1*B*) provided an estimate of the relative contribution of Na^+ and Ca^{2+} currents to the total inward current in normal PSS.

Voltage-dependent properties of Na^+ currents

In normal PSS (140 mM-Na^+) a loss of voltage control often occurred, seen as an all-or-none inward current with variable delay, and an instantaneous increase of current to maximal values in the *I–V* relation was observed in most cells (see Fig. 1*A*). To avoid this problem, extracellular [Na^+] was reduced from 140 to 20 mM by substitution of Na^+ with TEA. Under these conditions Na^+ currents showed a reduced amplitude, reversal potential of +26 mV, and a continuously graded *I–V* relation (Fig. 2). Figure 2*A* shows depolarization-activated Na^+ currents (recorded in 0·1 mM Cd^{2+} to inhibit Ca^{2+} currents) elicited by incremental voltage steps from a

holding potential of −100 mV. Na^+ currents showed graded activation, with current amplitude initially increasing and then decreasing with further depolarization, as expected from a reduction in the driving force as the Na^+ equilibrium potential is approached. The sodium *I–V* curve exhibited detectible activation at −40 mV,

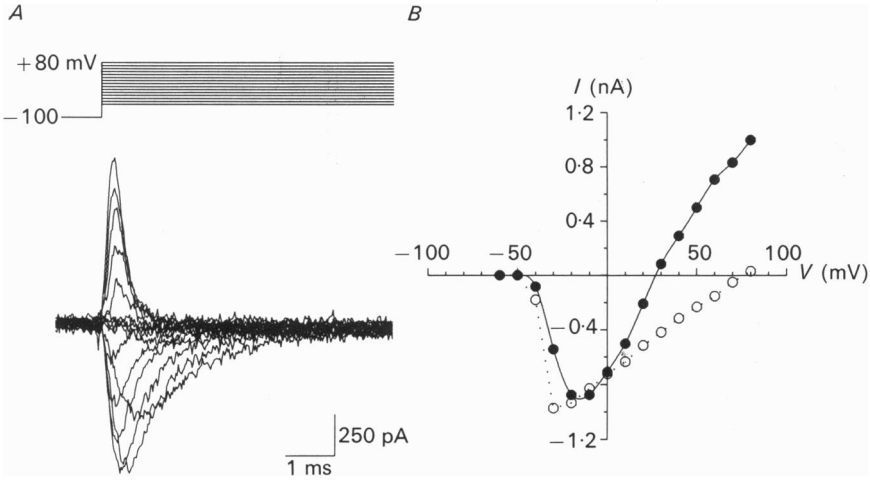

Fig. 2.Voltage-dependent Na^+ currents in rat intracardiac neurones. *A*, whole-cell Na^+ currents evoked by depolarizing test pulses (−60 to +80 mV) from a holding potential of −100 mV in the presence of 20 mM extracellular Na^+. The pipette solution contained 10 mM Na^+ and intracellular K^+ was replaced by arginine. Extracellular Na^+ (120 mM) was replaced isotonically by TEA to suppress outward currents through open K^+ channels and 0·1 mM Cd^{2+} was added to the bath solution to inhibit Ca^{2+} currents. *B*, *I–V* curves constructed from Na^+ currents recorded in 20 mM (●; extracellular Na^+ shown in *A*) and 140 mM extracellular Na^+ (○). The *I–V* curve obtained in the presence of 140 mM Na^+ was scaled 0·1 × to permit comparison with that obtained in 20 mM Na^+.

increasing to a maximum at −20 mV and decreasing in amplitude with further depolarization (Fig. 2*B*). Removal of extracellular Na^+ completely abolished the inward currents recorded in the presence of Cd^{2+}. The peak Na^+ current density calculated from the average measured cell capacitance of 15·4 ± 0·3 pF was 350·8 ± 18·3 pA/pF ($n = 16$) in normal PSS (140 mM Na^+).

The Na^+ activation curve was derived from this *I–V* curve and conductance calculated according to $g_{Na} = I_{Na}/(V_m - E_{Na})$, where g_{Na} is Na^+ conductance, I_{Na} is Na^+ current amplitude, V_m is the test potential and E_{Na} the reversal (zero current) potential of I_{Na}. Data points were normalized to the maximal conductance and fitted by the equation:

$$g_{Na} = g_{Na(max)}/\{1 + \exp[(V_h - V)/k]\}, \quad (1)$$

where V_h, the potential of half-maximal activation, was −25 mV, and k, the slope parameter, was 7·5 mV per e-fold change in conductance (Fig. 3, ●). In Fig. 3, ○ show the steady-state Na^+ inactivation curve. Data points represent peak current (normalized to the maximal value) evoked by step depolarizations to −10 mV from

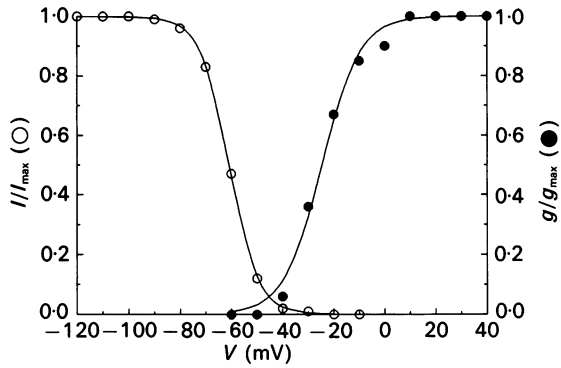

Fig. 3. Activation and steady-state inactivation of the Na^+ conductance (g_{Na}). The activation curve was determined by calculating g_{Na} at each test potential and normalized to the maximum g_{Na}. The data were fitted by eqn (1), with $V_h = -25$ mV and $k = 7{\cdot}5$ mV. The inactivation curve (h_∞) was determined by measuring peak amplitude of I_{Na} at −10 mV elicited from conditioning prepulses (5 s) of variable amplitude. Relative I_{Na} amplitudes were calculated and fitted with eqn (2) with $V_h = -61$ mV and $k = 5{\cdot}7$ mV.

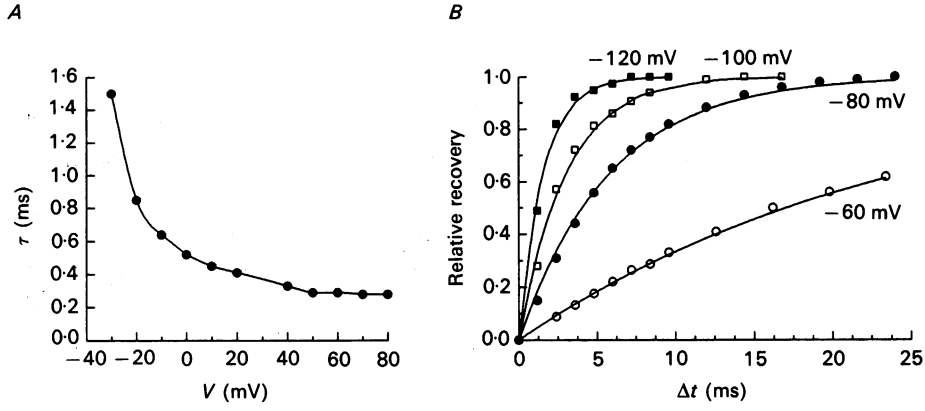

Fig. 4. *A*, voltage dependence of the onset of I_{Na} inactivation. The time course of decay of Na^+ currents recorded in 20 mM Na^+ was fitted with a single exponential function and the time constant of decay is plotted as a function of membrane potential. *B*, voltage dependence of recovery from inactivation. Test pulses to −20 mV were applied at varying intervals (Δt) and from different interpulse voltages (−60 to −120 mV) following prepulses to the same voltage. The relative recovery of Na^+ current (peak I_{Na} amplitude for the test pulse divided by that obtained for the prepulse) is plotted as a function of the interpulse interval (Δt). The curves represent the best fit of the data at each potential with a single exponential function.

holding potentials between −120 and −10 mV. The steady-state inactivation curve $h_\infty(V)$ also showed a sigmoidal dependence on voltage described by:

$$I_{Na} = I_{Na(max)}/\{1+\exp[(V-V_h)/k]\}, \quad (2)$$

where $V_h = -61$ mV and $k = 5{\cdot}7$ mV. The non-inactivated fraction of I_{Na} fell to zero at −30 mV and was maximal at about −90 mV.

Inactivation and recovery kinetics of Na^+ current

The time course for onset of inactivation during a depolarization was well fitted by a single exponential function at all membrane potentials. The time constant of decay (τ_h) decreased with increasing depolarization and the voltage dependence of average

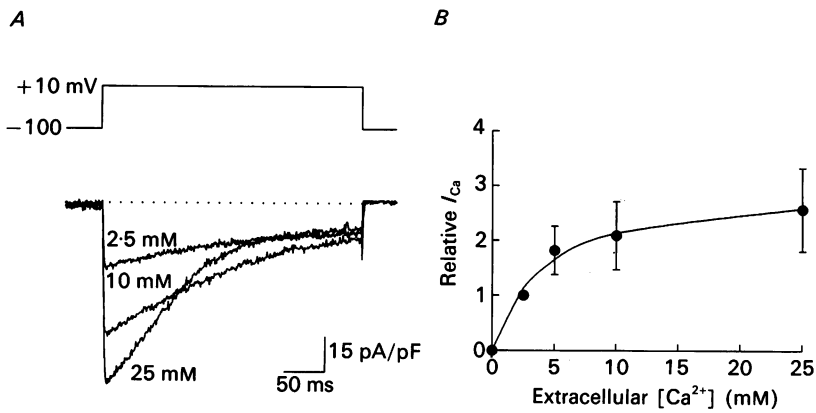

Fig. 5. Dependence of Ca^{2+} current amplitude and time course of inactivation on extracellular Ca^{2+} concentration. *A*, Ca^{2+} currents obtained in the same cell in 2·5, 10 or 25 mM extracellular Ca^{2+} by voltage steps which elicited maximum Ca^{2+} current from a holding potential of −100 mV. *B*, saturation of whole-cell Ca^{2+} current amplitude as a function of the extracellular Ca^{2+} concentration. ● represent the means ± S.E.M. peak I_{Ca} amplitude obtained in five cells in different extracellular [Ca^{2+}], normalized to that obtained in the presence of 2·5 mM Ca^{2+}. The curve of best fit according to the Michaelis–Menten equation had a dissociation constant, $K_d \approx 4$ mM.

τ_h is shown in Fig. 4*A*. The voltage- and time-dependence of recovery from inactivation was evaluated using a double-pulse protocol. Figure 4*B* plots for a typical neurone the relative peak Na^+ currents evoked by the test pulse as a function of the duration of the interpulse interval and holding potential. Inactivation was removed over a time course of milliseconds and the process was markedly voltage dependent. In each case, the time course is fitted by a single exponential function.

Depolarization-activated Ca^{2+} currents

Voltage-dependent Ca^{2+} currents (I_{Ca}) in rat parasympathetic cardiac neurones were detected by blocking Na^+ current with 300 nM TTX and K^+ currents were suppressed with either Cs^+ or arginine intracellularly plus 50 mM extracellular TEA. Figure 5 shows the relationship between the peak amplitude of the inward current and the extracellular [Ca^{2+}]. The current–concentration relationship saturated at [Ca^{2+}] above 10 mM and was fitted by a Michaelis–Menten curve with a dissociation constant of 4 mM (Fig. 5*B*). The peak Ca^{2+} current density in the presence of the normal 2·5 mM-extracellular Ca^{2+} was 44·8 ± 3·8 pA/pF ($n = 20$). The inward Ca^{2+} current was completely abolished when extracellular Ca^{2+} was replaced with Mg^{2+} (not shown). The time course of decay of I_{Ca} became faster as bath Ca^{2+} increased (Fig. 5*A*).

Ionic currents carried by Ca^{2+}, Ba^{2+} and Na^+ through open Ca^{2+} channels are

shown in Fig. 6. The time to peak of inward Ca^{2+} currents varied as a function of the test potential and was followed by a slow inactivation with ~ 50% inactivation during a 400 ms depolarizing pulse (Fig. 6*A*). The Ba^{2+} and Na^+ permeability of the underlying channels is demonstrated in Fig. 6*A*. Ba^{2+} currents were recorded after

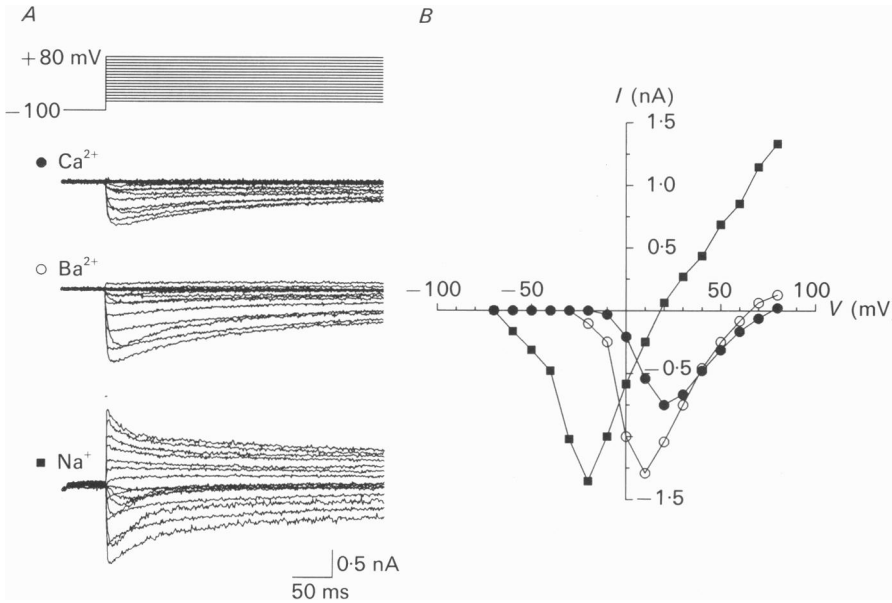

Fig. 6. Voltage-dependent ionic currents carried by Ca^{2+}, Ba^{2+} and Na^+ through Ca^{2+} channels. *A*, depolarization-activated whole-cell currents through Ca^{2+} channels carried by Ca^{2+}, Ba^{2+} and Na^+, evoked by step depolarizations (−70 to +80 mV) from a holding potential of −100 mV in one cell. The external solution contained 10 mM Ca^{2+}, 10 mM Ba^{2+} or 76 mM Na^+ (divalent cation free). *B*, *I–V* curves for peak Ca^{2+} (●), Ba^{2+} (○) and Na^+ (■) currents through open Ca^{2+} channels for data shown in *A*.

replacement of extracellular Ca^{2+} by Ba^{2+}, and Na^+ currents, in a divalent ion-free external solution containing 76 mM Na^+. The corresponding current–voltage relationships obtained for these Ca^{2+}, Ba^{2+} and Na^+ currents are shown in Fig. 6*B*. The threshold for activation of Ca^{2+} current was ~ −10 mV and was maximal at +20 mV. The Ca^{2+} current appeared to reverse at approximately +80 mV. This value is lower than the estimated Ca^{2+} equilibrium potential (~ +120 mV), suggesting that the Ca^{2+} channel may also be permeable to the major intracellular cation Cs^+. The outward currents obtained at membrane potentials positive to the reversal (zero current) potential were blocked by the addition of 0·1 mM $CdCl_2$ to the bath at a given membrane potential. Peak inward current amplitudes in Ba^{2+} were larger than those measured in Ca^{2+}, indicating that Ba^{2+} passes through the Ca^{2+}channel easier than Ca^{2+}. The *I–V* relationship was shifted to more negative potentials when extracellular Ca^{2+} was replaced with either Ba^{2+} or Na^+. This shift in the *I–V* relation with Ba^{2+} and Na^+ as charge carriers has been observed for calcium channels in other vertebrate cells (see Tsien, Hess, McCleskey & Rosenberg, 1987).

Voltage-dependent properties of Ca^{2+} currents

The voltage-dependent and kinetic properties of the Ca^{2+} current were examined in order to detect kinetic varieties of Ca^{2+} channels. In the majority of the neurones, the *I–V* curve exhibited a single maximum with either Ca^{2+} or Ba^{2+} as the charge

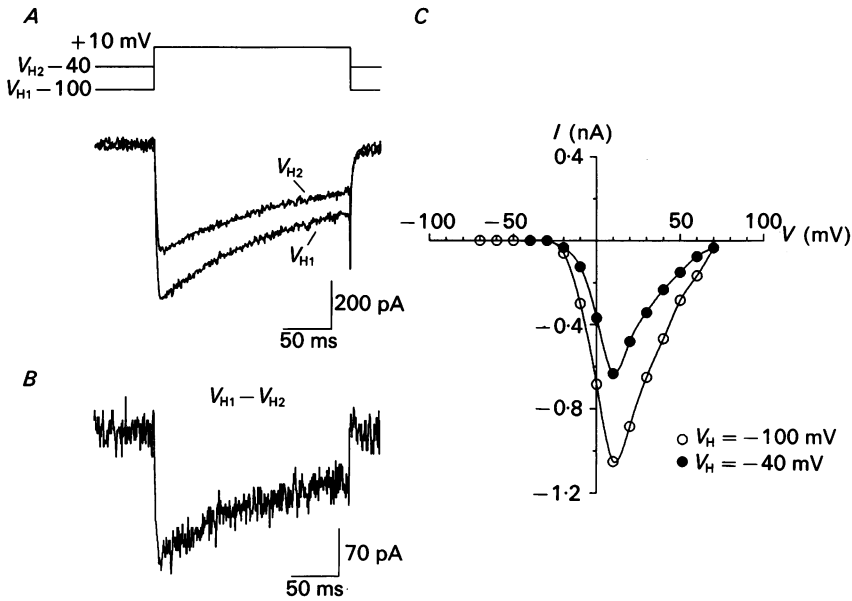

Fig. 7. Effect of holding potential on the whole-cell Ca^{2+} current. *A*, superimposed Ca^{2+} currents elicited with a 200 ms depolarization pulse to +10 mV from a holding potential of either −100 mV (V_{H1}) or −40 mV (V_{H2}). *B*, difference current obtained by subtracting the Ca^{2+} current recorded at a holding potential of −40 mV from that at −100 mV ($V_{H1} - V_{H2}$). *C*, *I–V* relations for Ca^{2+} currents recorded from a holding potential of either −40 or −100 mV.

carrier (see Fig. 6). Shifting the holding potential from −100 to −40 mV did not shift the voltage dependence of the currents (Fig. 7). These findings suggest that a low-threshold Ca^{2+} current (Fox, Nowycky & Tsien, 1987) was not detectable in the rat intracardiac parasympathetic neurones.

The voltage dependence of activation and inactivation of the Ca^{2+} conductance is shown in Fig. 8. The activation curve determined by calculating the relative Ca^{2+} conductance normalized to the maximum conductance from the I_{Ca}–*V* curve, was fitted by the Boltzmann equation with $V_h = -4$ mV and $k = 4{\cdot}2$ mV. The steady-state inactivation curve determined with test pulses to +20 mV was half-maximal at −38 mV and had a slope of 8·6 mV (Fig.8, ○). The slight overlap between the activation and inactivation curves for the Ca^{2+} conductance evoked at voltages between −20 and −10 mV indicates the presence of a small steady-state Ca^{2+} conductance in rat parasympathetic cardiac neurones.

The time course of inactivation of the inward I_{Ca} was fitted by the sum of two

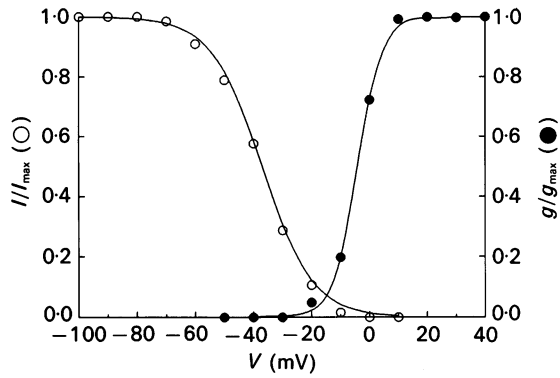

Fig. 8. Activation and steady-state inactivation of the Ca^{2+} conductance (g_{Ca}). The activation curve obtained by calculating g_{Ca} at each voltage and normalized to the maximum g_{Ca}. The relative conductance (●) was plotted as a function of the test potential and fitted according to eqn (1) with $V_h = -4$ mV and $k = 4{\cdot}2$ mV. The g_{Ca} inactivation curve was determined by measuring I_{Ca} evoked by test pulses to +20 mV from conditioning prepulses (5 s) at different membrane potentials. Relative g_{Ca} (○) was plotted as a function of the conditioning prepulse voltage and fitted by eqn (2) with $V_h = -38$ mV and $k = 8{\cdot}6$ mV.

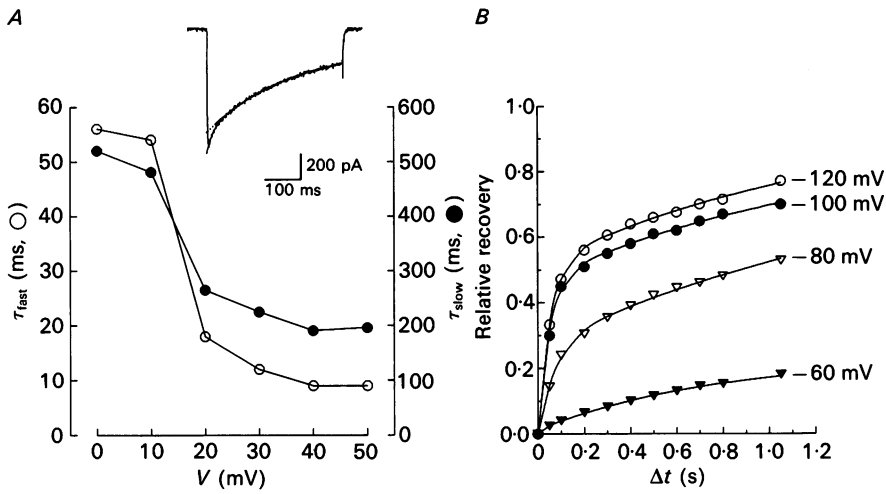

Fig. 9. Voltage dependence of inactivation kinetics of Ca^{2+} current. *A*, voltage dependence of the onset of inactivation of Ca^{2+} current during maintained depolarization. The time course of decay of I_{Ca} was fitted by the sum of two exponential functions whose time constants (τ_{fast} and τ_{slow}) are plotted as a function of voltage. Inset: I_{Ca} elicited by a voltage step to +20 mV from −100 mV. The time course of I_{Ca} decay was fitted by single (dotted line) and double exponential (continuous line) functions. *B*, voltage dependence of I_{Ca} recovery from inactivation determined using a double-pulse protocol. Test pulses to +20 mV were applied at varying intervals (Δt) from different potentials (−60 to −120 mV) after a 1 s prepulse to the same voltage (+20 mV). The relative recovery of I_{Ca} is plotted as a function of the interpulse interval (Δt), with steady-state I_{Ca} at the end of the prepulse being zero recovery and peak current during the prepulse being full recovery. The curves shown for each voltage represent the best fit of the data by the sum of two exponential functions.

exponential functions suggesting that at least two kinetic steps may be involved. The two time constants (τ_{fast} and τ_{slow}) differed by an order of magnitude. The voltage dependence of these time constants is plotted in Fig. 9*A*. Recovery from inactivation of I_{Ca} was examined using a double-pulse protocol where relative I_{Ca} amplitude was

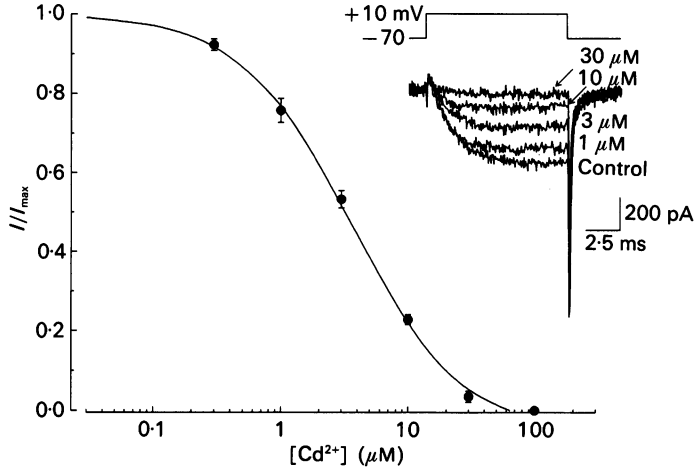

Fig. 10. Dose–response relationship for Cd^{2+} inhibition of Ca^{2+} currents. The ratio of the peak I_{Ca} amplitudes measured in the presence and absence of Cd^{2+} (I/I_{max}) is plotted against the extracellular Cd^{2+} concentration, with each point representing the means ± S.E.M. for six to fifteen different cells. The curve was drawn to fit the data using the equation, $I/I_{max} = 1-[Y_{min}/(1+[Cd^{2+}]/K_i]$ where $K_i = 3{\cdot}6\ \mu M$ and Y_{min} represents $I/I_{max} = 0$ with a maximum dose of Cd^{2+}. Inset: I_{Ca} elicited by depolarization to +10 mV from a holding potential of −70 mV in the indicated concentrations of Cd^{2+}.

plotted as a function of the interpulse interval (Δt). The time course of recovery from inactivation at different membrane potentials is shown in Fig. 9*B*. The rate of recovery was increased by hyperpolarization. The time course was fitted by the sum of two exponentials consistent with more than one kinetic step involved in the recovery process. Thus, the voltage- and time-dependent characteristics of I_{Ca} in rat parasympathetic cardiac neurones indicate the existence of a 'high-threshold' Ca^{2+} channel which exhibits at least two distinct kinetic steps in the inactivation of the channel.

Pharmacological antagonism of Ca^{2+} currents

The Ca^{2+} channel antagonist, Cd^{2+} reversibly inhibited I_{Ca} in a dose-dependent manner with half-maximal inhibition at 3·6 μM (Fig. 10). The Ca^{2+} current was modulated by the dihydropyridine agonist, Bay K 8644, and the antagonist, nifedipine (Fig. 11*A*). Bath application of Bay K 8644 (5 μM) increased I_{Ca} amplitude, whereas nifedipine (5 μM) decreased the amplitude of I_{Ca}. The effects of Bay K 8644 and nifedipine were partially reversible. The dose–response curve for inhibition of I_{Ca} by nifedipine is shown in Fig. 11*B* and was fitted with a K_i (concentration producing 50% inhibition of maximum response) of 3·4 μM. The

inhibition of I_{Ca} by nifedipine was incomplete, limited to 67% inhibition at nifedipine concentrations higher than 30 μM, suggesting that only a fraction of the underlying channels is dihydropyridine-sensitive.

The peptide toxin, ω-conotoxin (ω-CGTX), irreversibly inhibited the Ca^{2+} current. Bath application of ω-CGTX concentrations $\geqslant$ 300 nM produced a block that saturated

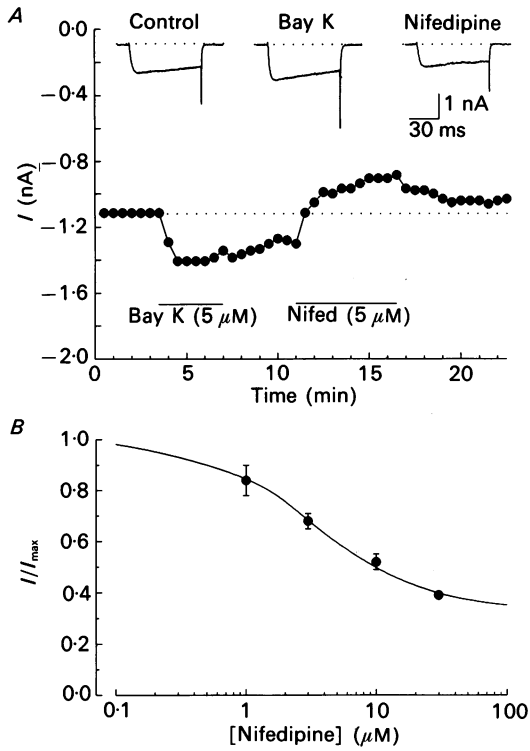

Fig. 11. Actions of dihydropyridine on Ca^{2+} currents. *A*, peak amplitude of I_{Ca} measured before, during and after bath application of 5 μM Bay K 8644 or 5 μM nifedipine as a function of time. Inset: representative Ca^{2+} currents elicited by test pulses to +10 mV from a holding potential of −70 mV before and after applying 5 μM Bay K 8644 or 5 μM nifedipine. *B*, dose–response curve for nifedipine inhibition of Ca^{2+} current. Each point represents the mean relative I_{Ca} amplitude ±S.E.M. determined by a voltage step from −70 to +10 mV in the presence of different concentrations of nifedipine ($n = 3$). The fitted curve had a $K_i = 3{\cdot}4$ μM and $Y_{min} = 0{\cdot}33$.

at about 30% of control (Fig. 12*A*), suggesting that a fraction of the channels is resistant to ω-CGTX. An experiment in which the inhibition of I_{Ca} by ω-CGTX and nifedipine was examined on the same neurone is shown in Fig. 12*B*. Ca^{2+} current amplitude was initially reduced by ~ 70% by a high dose of ω-CGTX (300 nM), the remaining I_{Ca} was further inhibited to 15% of control when 20 μM nifedipine was applied. These data suggest that the block of Ca^{2+} channels by dihydropyridine and ω-CGTX may be partially additive, however, the simultaneous addition of maximal doses of ω-CGTX and nifedipine did not completely block I_{Ca} in any of the six neurones examined. The ω-CGTX- and nifedipine-resistant component of I_{Ca} was

blocked by 100 μM Cd^{2+}. High concentrations (> 30 μM) of the 1,4-dihydropyridine antagonist, amlodipine, also blocked the Ca^{2+} current remaining in a saturating dose of ω-CGTX (not shown).

The difference in the efficacy of nifedipine and amlodipine may be related to their structure and accessibility to the dihydropyridine receptor site or to a non-specific

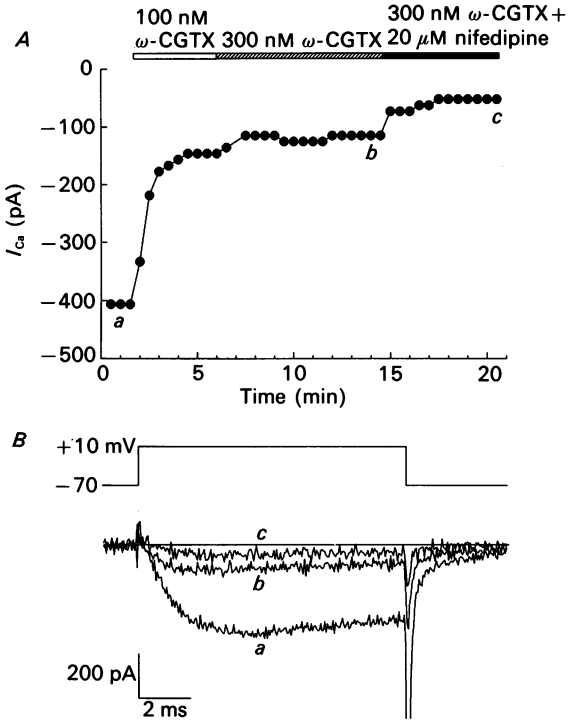

Fig. 12. Incomplete block of Ca^{2+} current by ω-CGTX and nifedipine. *A*, peak amplitude of I_{Ca} obtained in the absence and presence of either ω-CGTX or ω-CGTX plus nifedipine at the concentrations indicated as a function of time. The Ca^{2+} current was elicited by the voltage step shown in *B*. *B*, incomplete block of Ca^{2+} current by maximal doses of ω-CGTX and nifedipine. Depolarization-activated Ca^{2+} currents obtained in the absence (*a*) and presence of either 300 nM ω-CGTX (*b*) or ω-CGTX plus 20 μM nifedipine (*c*). I_{Ca} was initially reduced approximately 75% by 300 nM ω-CGTX and subsequent bath application of 20 μM nifedipine blocked an additional 10% of I_{Ca}, leaving about 15% of the original current resistant to both Ca^{2+} channel antagonists.

effect of high concentrations of amlodipine. These results suggest that the Ca^{2+} current in rat parasympathetic cardiac neurones consist of at least three distinct components: a nifedipine-sensitive, an ω-CGTX-sensitive, and a nifedipine- and ω-CGTX-insensitive component. There is overlap in the inhibition of I_{Ca} by nifedipine and ω-CGTX, since each drug can block over half the I_{Ca}, and the fraction of I_{Ca} blocked by the combination of both drugs is less than that expected if both drugs had independent sites of action (see Fig. 12*B*). Amiloride (30 μM), a potent antagonist of T-type Ca^{2+} channels in chick dorsal root ganglion neurones and neuroblastoma cells

(Tang, Presser & Morad, 1988; Carbone, Sher & Clementi, 1990) and of neurally evoked transmitter release in rat parasympathetic ganglia (Seabrook & Adams, 1989) had no effect on Ca^{2+} current amplitude. This result together with the lack of a significant I_{Ca} component in weakly depolarized cells (Fig. 7), suggest the absence of a low threshold, T-type Ca^{2+} current in the cell bodies of these neurones.

DISCUSSION

Voltage-dependent Na^+ current

The voltage- and time-dependent properties of the Na^+ conductance in rat parasympathetic cardiac neurones are similar to those reported for the Na^+ conductance in rat sympathetic neurones (Belluzzi & Sacchi, 1986; Schofield & Ikeda, 1988) but different from those reported for bullfrog parasympathetic intracardiac neurones (Clark, Tse & Giles, 1990). The activation parameters for the Na^+ conductance in rat parasympathetic cardiac neurones ($V_h = -25$ mV, $k =$ 7·5 mV) may be compared to those reported for rat sympathetic neurones ($V_h = -21$ mV, $k = 6{\cdot}5$ mV; Belluzzi & Sacchi, 1986). The inactivation properties of the Na^+ conductance in rat parasympathetic cardiac neurones ($V_h = -61$ mV, $k =$ 5·7 mV) are also similar to those found in rat sympathetic neurones of the intact rat superior cervical ganglion (SCG) ($V_h = -56$ mV, $k = 6{\cdot}5$ mV; Belluzzi & Sacchi, 1986) and the acutely isolated rat SCG ($V_h = -59$ mV and $k = 7{\cdot}6$ mV; Schofield & Ikeda, 1988). The onset and recovery from inactivation of the Na^+ current in rat parasympathetic neurones also had time courses and voltage dependence similar to those reported for rat sympathetic neurones (Belluzzi & Sacchi, 1986). The time course of recovery from inactivation, with a time constant of 13 ms at -60 mV, is also consistent with the maximal firing frequency (20 Hz) of these neurones in response to repetitive trains of current pulses. The slow inactivation process that has been described in SCG sensory neurones (Belluzzi & Sacchi, 1986) and bullfrog sympathetic neurones (Jones, 1987) was not investigated in this study. The overlap between Na^+ activation and inactivation curves suggests a persistent contribution of Na^+ influx to the resting membrane potential, compatible with the relatively high resting membrane permeability to Na^+ ($P_{Na}/P_K = 0{\cdot}12$) in rat parasympathetic cardiac neurones (Xu & Adams, 1992).

The TTX sensitivity of the depolarization-activated Na^+ current in rat parasympathetic neurones, with complete blockade at 300 nM TTX, is similar to that found in rat sympathetic neurones (Belluzzi & Sacchi, 1986; Schofield & Ikeda, 1988). In contrast, bullfrog parasympathetic (Clark *et al.* 1990) and sympathetic (Jones, 1987) neurones as well as rat sensory neurones (Kostyuk *et al.* 1981*b*; Ikeda *et al.* 1986; Ikeda & Schofield, 1987) exhibit a TTX-insensitive Na^+ current.

Voltage-dependent Ca^{2+} current

Rat parasympathetic neurones exhibit a robust voltage-dependent Ca^{2+} conductance which activates upon step depolarizations beyond -20 mV with maximal activation at $+20$ mV. Half-maximal activation (V_h) occurred at -4 mV with a slope of 4·2 mV, which is similar to the values measured for activation of L-type Ca^{2+} channels in chick sensory neurones (Fox *et al.* 1987). Changing the holding potential

from −100 to −40 mV did not alter the voltage dependence of I_{Ca} (Fig. 7), indicating the absence of a low-threshold I_{Ca} in the soma of rat parasympathetic neurones (cf. Akasu *et al.* 1990). This finding is consistent with the lack of blockade by amiloride. Low-threshold Ca^{2+} currents are also absent from the somata of frog parasympathetic intracardiac neurones (Clark *et al.* 1990) and rat sympathetic neurones (Marrion *et al.* 1987; Wanke, Ferroni, Malgaroli, Ambrosini, Pozzan & Meldolesi, 1987; Hirning *et al.* 1988; Schofield & Ikeda, 1988).

At least three major types of Ca^{2+} channels, T, N and L, have been reported in a variety of mammalian central and peripheral neurones (for review see Tsien *et al.* 1987; Tsien, Lipscombe, Madison, Bley & Fox, 1988; Bean, 1989). While there is general agreement on the characterization of low threshold, T-type Ca^{2+} channels, discrimination between the high-threshold, N- and L-type Ca^{2+} channels is less clear. Although most studies confirm the existence of two types of high-threshold Ca^{2+} channels in vertebrate neurones, the distinction between N- and L-type Ca^{2+} channels has been questioned due to the overlap in the voltage- and time-dependence of activation and inactivation (Hirning *et al.* 1988; Swandulla & Armstrong, 1988; Aosaki & Kasai, 1989; Plummer, Logothetis & Hess, 1989). It has been proposed that high-threshold Ca^{2+} current might be distinguished by their relative sensitivities to ω-CGTX and dihydropyridine (Aosaki & Kasai, 1989; Plummer *et al.* 1989). Recent studies have revealed three pharmacologically distinct components of high-threshold Ca^{2+} current, dihydropyridine-sensitive, ω-CGTX-sensitive and a component resistant to both antagonists (Mogul & Fox, 1991; Regan, Sah & Bean, 1991).

The kinetic and pharmacological properties of the whole-cell I_{Ca} in rat parasympathetic cardiac neurones suggest the existence of more than one type of high-threshold Ca^{2+} channel. The voltage-dependent kinetics of onset, and recovery from, inactivation were both described by the sum of two exponential functions with time constants differing by about an order of magnitude (Fig. 9), consistent with the existence of more than one type of Ca^{2+} channel in rat parasympathetic neurones. Pharmacological studies provided further evidence for a heterogeneous population of Ca^{2+} channels in these neurones. The whole-cell Ca^{2+} current was sensitive to nifedipine and ω-CGTX with a saturating dose of each drug inhibiting more than half the total I_{Ca}. This finding suggests that there is considerable overlap in the inhibition of I_{Ca} by these two Ca^{2+} channel antagonists. The Ca^{2+} current resistant to both nifedipine and ω-CGTX accounted for approximately 15% of the total Ca^{2+} current and was blocked by 100 μM Cd^{2+} (Fig. 12). This nifedipine- and ω-CGTX-insensitive current is similar to a Ca^{2+} current recently reported in rat sympathetic neurones (Regan *et al.* 1991).

The Ca^{2+} channels in the soma of rat parasympathetic neurones exhibit a different sensitivity to Ca^{2+} channel antagonists compared to those Ca^{2+} channels of presynaptic nerve terminals mediating neurally evoked neurotransmitter release (Seabrook & Adams, 1989). Taken together, these results are consistent with an asymmetrical distribution of different Ca^{2+} channel types between the cell body and presynaptic terminal as reported in frog sympathetic neurones (Lipscombe, Madison, Poenie, Reuter, Tsien & Tsien, 1988).

We thank Drs Ellen Barrett, Wolfgang Nonner and Thomas Nutter for their helpful comments on a draft of this manuscript. This work was supported by National Institutes of Health grant HL 35422 to D. J. Adams.

REFERENCES

ADAMS, D. J. & XU, Z.-J. (1989). Norepinephrine and GTPγS inhibit a calcium conductance and activate a non-selective cation conductance in rat parasympathetic cardiac neurons. *Journal of General Physiology* **94**, 1–2 a.

AKASU, T., TSURUSAKI, M. & TOKIMASA, T. (1990). Reduction of the N-type calcium current by noradrenaline in neurones of rabbit vesical parasympathetic ganglia. *Journal of Physiology* **426**, 439–452.

ALLEN, T. G. J. & BURNSTOCK, G. (1987). Intracellular studies of the electrophysiological properties of cultured intracardiac neurones of the guinea-pig. *Journal of Physiology* **388**, 349–366.

AOSAKI, T. & KASAI, H. (1989). Characterization of two kinds of high-voltage-activated Ca-channel currents in chick sensory neurons. Differential sensitivity to dihydropyridines and omega-conotoxin GVIA. *Pflügers Archiv* **414**, 150–156.

BEAN, B. P. (1989). Classes of calcium channels in vertebrate cells. *Annual Review of Physiology* **51**, 367–384.

BELLUZZI, O. & SACCHI, O. (1986). A quantitative description of the sodium current in the rat sympathetic neurone. *Journal of Physiology* **380**, 275–291.

BELLUZZI, O. & SACCHI, O. (1989). Calcium currents in the normal adult rat sympathetic neurone. *Journal of Physiology* **412,** 493–512.

BOSSU, J.-L. & FELTZ, A. (1986). Inactivation of the low-threshold transient calcium current in rat sensory neurones: evidence for a dual process. *Journal of Physiology* **376**, 341–357.

BOSSU, J.-L., FELTZ, A. & THOMANN, J. M. (1985). Depolarization elicits two distinct calcium currents in vertebrate sensory neurones. *Pflügers Archiv* **403**, 360–368.

CARBONE, E. & LUX, H. D. (1987). Kinetics and selectivity of a low voltage-activated calcium current in chick and rat sensory neurones. *Journal of Physiology* **386**, 547–570.

CARBONE, E., SHER, E. & CLEMENTI, F. (1990). Ca currents in human neuroblastoma IMR32 cells: kinetics, permeability and pharmacology. *Pflügers Archiv* **416**, 170–179.

CLARK, R. B., TSE, A. & GILES, W. R. (1990). Electrophysiology of parasympathetic neurones isolated from the interatrial septum of bull-frog heart. *Journal of Physiology* **427**, 89–125.

FEDULOVA, S. A., KOSTYUK, P. G. & VESELOVSKY, N. S. (1985). Two types of calcium channels in the somatic membrane of new-born rat dorsal root ganglion neurones. *Journal of Physiology* **359**, 431–446.

FENWICK, E. M., MARTY, A & NEHER, E. (1982). Sodium and calcium currents in bovine chromaffin cells. *Journal of Physiology* **331**, 599–635.

FORSCHER, P. & OXFORD, G. S. (1985). Modulation of calcium channels by norepinephrine in internally dialyzed avian sensory neurons. *Journal of General Physiology* **85**, 743–763.

FOX, A. P., NOWYCKY, M. C. & TSIEN, R. W. (1987). Kinetic and pharmacological properties distinguishing three types of calcium currents in chick sensory neurones. *Journal of Physiology* **394**, 149–172.

HIRNING, L. D., FOX, A. P., MCCLESKEY, E. W., OLIVERA, B. M., THAYER, S. A., MILLER, R. J. & TSIEN, R. W. (1988). Dominant role of N-type Ca^{2+} channels in evoked release of norepinephrine from sympathetic neurons. *Science* **239**, 57–61.

IKEDA, S. R. & SCHOFIELD, G. G. (1987). Tetrodotoxin-resistant sodium current of rat nodose neurones: monovalent cation selectivity and divalent cation block. *Journal of Physiology* **389**, 255–270.

IKEDA, S. R., SCHOFIELD, G. G. & WEIGHT, F. F. (1986). Na^+ and Ca^{2+} currents of acutely isolated adult rat nodose ganglion cells. *Journal of Neurophysiology* **55**, 527–539.

JONES, S. W. (1987). Sodium currents in dissociated bull-frog sympathetic neurones. *Journal of Physiology* **389**, 605–627.

KOSTYUK, P. G., SHUBA, M. F. & SAVCHENKO, A. N. (1988). Three types of calcium channels in the membrane of mouse sensory neurones. *Pflügers Archiv* **411**, 661–669.

KOSTYUK, P. G., VESELOVSKY, N. S. & FEDULOVA, S. A. (1981*a*). Ionic currents in the somatic membrane of rat dorsal root ganglion neurons – II. Calcium currents. *Neuroscience* **6**, 2431–2437.

KOSTYUK, P. G., VESELOVSKY, N. S. & TSYNDRENKO, A. Y. (1981*b*). Ionic currents in the somatic membrane of rat dorsal root ganglion neurons – I. Sodium currents. *Neuroscience* **6**, 2423–2430.

LIPSCOMBE, D., MADISON, D. V., POENIE, M., REUTER, H., TSIEN, R. Y. & TSIEN, R. W. (1988). Spatial distribution of calcium channels and cytosolic calcium transients in growth cones and cell bodies of sympathetic neurons. *Proceedings of the National Academy of Sciences of the USA* **85**, 2398–2402.

MARRION, N. V., SMART, T. G. & BROWN, D. A. (1987). Membrane currents in adult rat superior cervical ganglia in dissociated tissue culture. *Neuroscience Letters* **77**, 55–60.

MOGUL, D. & FOX, A. P. (1991). Evidence for multiple types of Ca^{2+} channels in acutely isolated hippocampal CA3 neurones of the guinea-pig. *Journal of Physiology* **433**, 259–281.

PLUMMER, M. R., LOGOTHETIS, D. E. & HESS, P. (1989). Elementary properties and pharmacological sensitivities of calcium channels in mammalian peripheral neurons. *Neuron* **2**, 1453–1463.

REGAN, L. J., SAH, D. W. Y. & BEAN, B. P. (1991). Ca^{2+} channels in rat central and peripheral neurons: high-threshold current resistant to dihydropyridine blockers and ω-conotoxin. *Neuron* **6**, 269–280.

SCHOFIELD, G. G. & IKEDA, S. R. (1988). Sodium and calcium currents of acutely isolated adult rat superior cervical ganglion neurons. *Pflügers Archiv* **441**, 481–490.

SEABROOK, G. R. & ADAMS, D. J. (1989). Inhibition of neurally-evoked transmitter release by calcium channel antagonists in rat parasympathetic ganglia. *British Journal of Pharmacology* **97**, 1125–1136.

SEABROOK, G. R., FIEBER, L. A. & ADAMS, D. J. (1990). Neurotransmission in neonatal rat cardiac ganglion in situ. *American Journal of Physiology* **259**, H997–1005.

SWANDULLA, D. & ARMSTRONG, C. M. (1988). Fast deactivating calcium channels in chick sensory neurons. *Journal of General Physiology* **92**, 197–218.

TANG, C.-M., PRESSER, F. & MORAD, M. (1988). Amiloride selectivity blocks the low threshold (T) calcium channel. *Science* **240**, 213–215.

TSIEN, R. W., HESS, P., MCCLESKEY, E. W. & ROSENBERG, R. L. (1987). Calcium channels: mechanisms of selectivity, permeation, and block. *Annual Review of Biophysics and Biophysical Chemistry* **16**, 265–290.

TSIEN, R. W., LIPSCOMBE, D., MADISON, D. V., BLEY, K. R. & FOX, A. P. (1988). Multiple types of neuronal calcium channels and their selective modulation. *Trends in Neurosciences* **11**, 431–438.

TSURUSAKI, M., NISHIMURA, T. & AKASU, T. (1990). Properties of voltage-dependent barium currents in neurons of pelvic parasympathetic ganglia of rabbit. *Japanese Journal of Physiology* **40**, 423–427.

WANKE, E., FERRONI, A., MALGAROLI, A., AMBROSINI, A., POZZAN, T. & MELDOLESI, J. (1987). Activation of muscarine receptor selectivity inhibits a rapidly inactivated Ca^{2+} current in rat sympathetic neurons. *Proceedings of the National Academy of Sciences of the USA* **84**, 4313–4317,

XI, X., THOMAS, J. X., RANDALL, W. C. & WURSTER, R. D. (1991). Intracellular recordings from canine intracardiac ganglion cells. *Journal of the Autonomic Nervous System* **32**, 177–182.

XU, Z.-J. & ADAMS, D. J. (1992). Resting membrane potential and potassium currents in cultured parasympathetic neurones from rat intracardiac ganglia. *Journal of Physiology* **456**, 405–424.